Optimal Design Method of Three-Phase Rectifier with Near-Sinusoidal Input Currents

Zhong Chen, Yingpeng Luo, YinyuZhu and Shunqing Wang
Aero-Power Sci-tech Center
Nanjing University of Aeronautics & Astronautics
Nanjing, 210016, P.R. China
Email: chenz@nuaa.edu.cn

Abstract—**In this paper, an optimal design method of three-phase rectifier with near-sinusoidal input currents (RNSIC) is proposed. By using the proposed method, high power factor could be achieved as well as low input current harmonics, making the converter more practical. Moreover, based on the operation principle analysis of RNSIC, characteristic of the rectifier is discussed. Experimental results form three prototypes with different specifications are shown to confirm the validity of the analysis and the feasibility of the proposed optimal design method.**

I. INTRODUCTION

Due to the rapid development of the power electronic technology, a number of power electronic equipments have been utilized. The conventional uncontrolled three-phase rectifiers with dc-side *C* filter are widely used as interface circuits between the utility grid and the power electronic equipments for their simplicity and reliability.

A large amount of harmonic components of current drawn from ac mains by the nonlinear load bring serious problems [1]. Active power filter (APF) technology has attracted more and more attention for its excellent harmonic filtering performance. However, the active filters are slightly inferior in cost and efficiency to the passive filters [2].

The passive power factor correction (PPFC) technology is more widely used for its low cost, high reliability and simple fabrication. Traditional method to improve three-phase power factor is using passive LC filters, which can be placed in ac side or dc side of the rectifiers. However, ac-side LC filter bring about dc voltage varying in a wide range and dc-side LC filter hardly obtain satisfactory performance [3], [4]. At present, some other PPFC technologies have been proposed and utilized. Multiple pulse rectifiers eliminate low-order harmonics through autotransformer, making the input current near-sinusoidal [5]-[7]. Rectifiers applying current injection contribute to the reduction of other harmonics present in input current, where the frequency of the injecting current is equal to the triple of the line frequency [8], [9]. Novel topology rectifiers, such as three-phase diode rectifiers with LC resonance in commercial frequency [10], three-phase rectifier with near sinusoidal input currents (RNSIC) have caught increasing attention in recent years [11]-[14].

RNSIC was proposed by D. Alexa in [13] in 2004. Compared with the conventional three-phase full-bridge rectifier with passive filter, the RNSIC has following attractive characteristics: sinusoidal input current for large variations of the load, lower size volume and cost of the passive components. But the design method given in [13] is not precise theoretically or is presented without enough derivation details, e.g., the reason why the values of inductors L and capacitors *C* fulfill the relation $0.05 \le LC\omega^2 \le 0.1$ is not explained. As such, an interested reader will not feel comfortable to use them for design purposes. All above facts limit the application of RNSIC.

This paper analyzes the operation principle of RNSIC in detail. Based on the analysis, a criterion to determine the operation mode of RNSIC converter is given. Furthermore, a time-weighted-averaging method valid for the parameter design of the rectifier is proposed, achieving near sinusoidal input currents and near unity displacement factor. According to the proposed method, optimal value of the passive components will be obtained, making RNSIC more practical. Three prototypes working in different operation modes are built and tested to verify the validity of the analysis and the feasibility of the method.

II. OPERATION PRINCIPLE

Fig.1 shows the configuration of RNSIC, which is composed of three series inductors L_u, L_v, L_w of equal inductance values *L* and six commutation capacitors C_1-C_6 of equal capacitance values *C*, where C_d is the output filter capacitor.

The phase voltages and input currents are supposed as follows:

This work was supported by Doctoral Fund of Ministry of Education of China under Award 200802871033 and Aeronautical Science Foundation of China under Award 2009ZC52030.

$$
\begin{aligned}
e_u &= U_m \sin \omega t & i_u &= I_m \sin \omega t \\
e_v &= U_m \sin(\omega t - \frac{2}{3}\pi) & i_v &= I_m \sin(\omega t - \frac{2}{3}\pi) \\
e_w &= U_m \sin(\omega t + \frac{2}{3}\pi) & i_w &= I_m \sin(\omega t + \frac{2}{3}\pi)
\end{aligned} \qquad (1)
$$

Where U_m is the amplitude of phase voltage, I_m is the amplitude of input current.

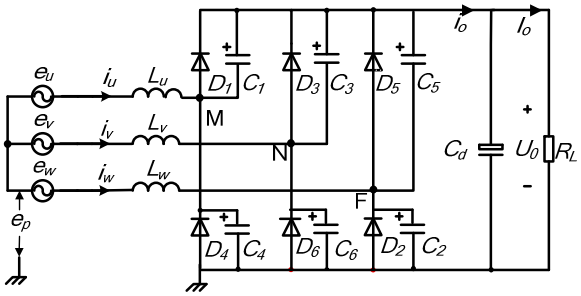

Figure 1. Topology of three-phase rectifier with near sinusoidal input currents.

In order to analyze the operation principle, the following assumptions are made:

- ideal diodes and passive components
- stead state already

Different durations of the current charging the commutation capacitor, which vary with the load, determine the distinct operation modes of the rectifier: large current mode, medium current mode and small current mode.

The duration of the current charging or discharging the capacitors is defined as t_1. Because capacitors begin to charge or discharge when the input currents cross zero, the conduction intervals of each diodes equal to $\pi/\omega - t_1$ due to the parallel connection of the capacitors and diodes.

In small current mode ($2\pi/3<\omega t_1<\pi$), none or one diode is conducting at any time. The conduction intervals of diode increase when the load current increases, as well as t_1 decreases. Rectifier changes into the medium current mode ($\pi/3<\omega t_1<2\pi/3$), in which one or two diodes are conducting. With the load current increasing continuously, rectifier changes into the large current mode ($0<\omega t_1<\pi/3$), in which two or three diodes are conducting. The waveforms of the phase currents and conduction intervals of the diodes are shown in Fig. 2(a), 3(a) and 4(a), from which differences among the three modes can be deduced.

Fig. 2(b), 3(b) and 4(b) illustrate the dc-side current i_o of the rectifiers working in different modes. Current i_o is discontinuous when the rectifier is working in the small current mode, whereas i_o become a 12-pulse waveform when the rectifier is working in the medium current mode and large current mode.

In what follows, operation principle of RNSIC working in the medium current mode will be discussed in detail.

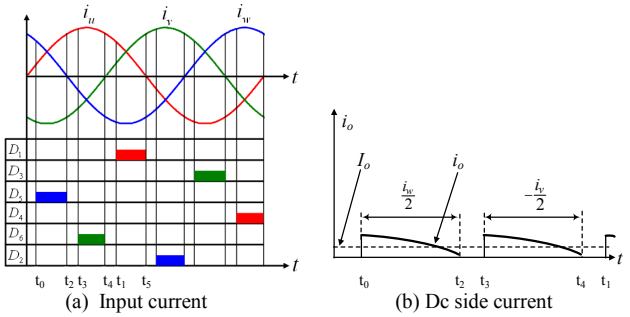

(a) Input current (b) Dc side current

Figure 2. Key waveforms of RNSIC working in small current mode.

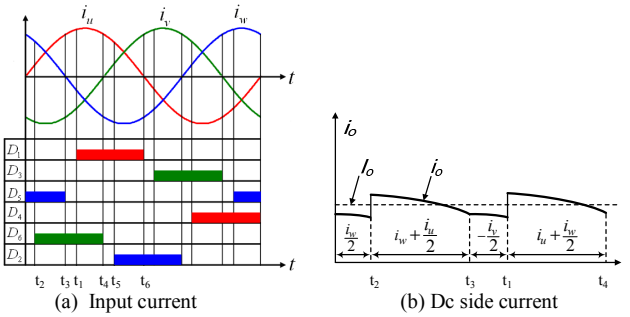

(a) Input current (b) Dc side current

Figure 3. Key waveforms of RNSIC working in medium current mode.

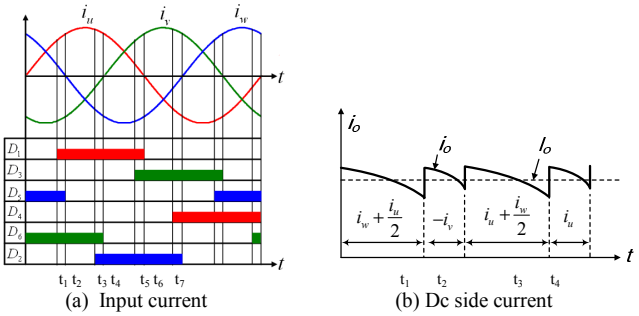

(a) Input current (b) Dc side current

Figure 4. Key waveforms of RNSIC working in large current mode.

A. *Medium Current Mode*

As Fig. 5 shows, four different operation stages exist in the medium current mode.

Stage 1 [0, t_2]: Prior to 0, D_4 and D_5 conducts, $u_{c4}=0$, $u_{c1}=U_o$. The input current i_v which is negative, charges the capacitor C_3 and discharges the capacitor C_6, simultaneously.

In the stage, the input current i_u which becomes positive at time point 0 charges the capacitor C_4 and discharges the capacitor C_1, and diode D_5 keeps conducting, as shown in Fig.5 (a). In this stage, the dc side current of the rectifier i_o is given by

$$
i_o = i_u/2 + i_v/2 + i_w = i_w/2 \qquad (2)
$$

Stage 2 [t_2, t_3]: At time point t_2 when the voltage across C_6 reaches zero, diode D_6 starts conducting. In the stage, the input current i_u which is positive keeps charging the capacitor C_4 and discharging the capacitor C_1, simultaneously. In this stage, the dc side current of the rectifier i_o is given by

$$i_o = i_w + i_u / 2 \tag{3}$$

Diode D_5 gets blocked at time point t_3 (corresponding to $\pi / 3\omega$), when current i_w crosses zero, indicating the end of stage 2.

Stage 3 [t_3, t_1]: At time point t_3, the input current i_w whose direction is changed into negative, begin to charge the capacitor C_5 and discharges the capacitor C_2, simultaneously. In the stage, the input current i_u which is positive keeps charging the capacitor C_4 and discharging the capacitor C_1. Diode D_6 keeps conducting, as shown in Fig. 5(c). In this stage, the dc side current of the rectifier i_o is given by

$$i_o = i_u / 2 + i_w / 2 = -i_v / 2 \tag{4}$$

Stage 4 [t_1, t_4]: At time point t_1, the voltage across C_1 reaches zero, diode D_1 starts conducting. In the stage, the input current i_w which is negative keeps charging the capacitor C_5 and discharging the capacitor C_2, simultaneously. In this stage, the dc side current of the rectifier i_o is given by

$$i_o = i_u + \frac{1}{2} i_w \tag{5}$$

Diode D_6 gets blocked at time point t_4 (corresponding to $2\pi / 3\omega$), when current i_v crosses zero, indicating the end of stage 4.

The dc side current i_o of RNSIC working in the medium current mode is given in Fig. 3(b). The output current I_o, the mean value of i_o, could be expressed as follow:

$$\begin{aligned} I_o = \frac{3}{2\pi}[&\int_0^{\omega t_1 - \frac{\pi}{3}} \frac{1}{2} i_w d\omega t + \int_{\omega t_1 - \frac{\pi}{3}}^{\frac{\pi}{3}} (i_w + \frac{1}{2} i_u) d\omega t \\ &+ \int_{\frac{\pi}{3}}^{\omega t_1} -\frac{1}{2} i_v d\omega t + \int_{\omega t_1}^{\frac{2\pi}{3}} (i_u + \frac{1}{2} i_w) d\omega t] \end{aligned} \tag{6}$$

The equation simplifies to

$$I_o = \frac{3}{2\pi}[I_m (1 + \cos \omega t_1)] \tag{7}$$

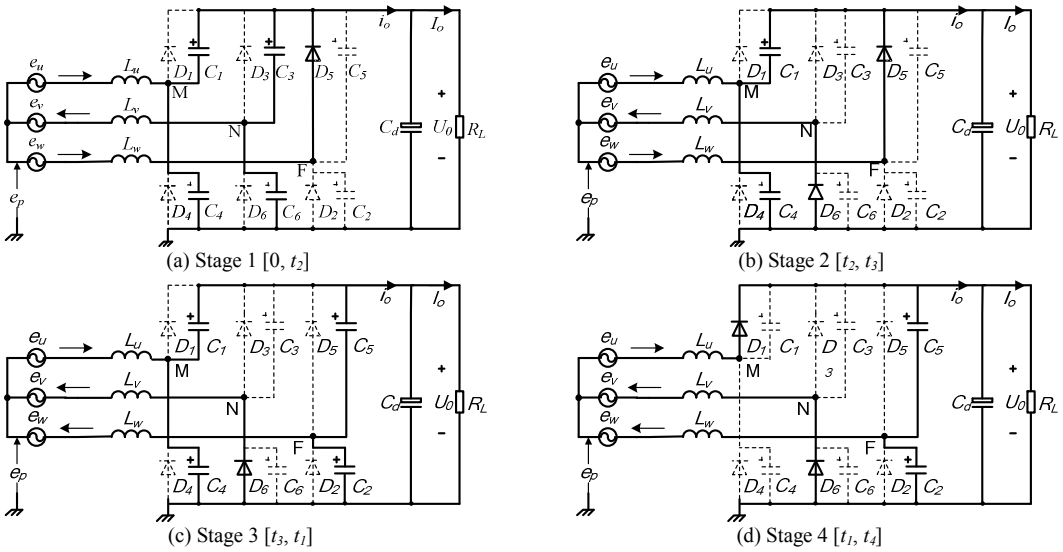

Figure 5. Equlicalent operation stage circuits of RNSIC working in medium current mode.

B. *Small and Large Current Mode*

As Fig. 3 and 4 depict, none or one diode conducts in the small current mode and two or three diodes conducts in the large current mode. Operation principle of the rectifier in these two operation modes could be derived by using the same analysis.

The output current I_o in the small current mode could be expressed as follow:

$$\begin{aligned} I_o &= \frac{3}{2\pi}(\int_{\omega t_1 - \frac{2}{3}\pi}^{\frac{\pi}{3}} \frac{1}{2} i_w d\omega t + \int_{\omega t_1 - \frac{\pi}{3}}^{\frac{2\pi}{3}} -\frac{1}{2} i_v d\omega t) \\ &= \frac{3}{2\pi}[I_m (1 + \cos \omega t_1)] \end{aligned} \tag{8}$$

The output current I_o in the large current mode could be expressed as follow:

$$\begin{aligned} I_o = \frac{3}{2\pi}[&\int_0^{\omega t_1} (i_w + \frac{1}{2} i_u) d\omega t + \int_{\omega t_1}^{\frac{\pi}{3}} -\frac{1}{2} i_v d\omega t \\ &+ \int_{\frac{\pi}{3}}^{\omega t_1 + \frac{\pi}{3}} (i_u + \frac{1}{2} i_w) d\omega t + \int_{\omega t_1 + \frac{\pi}{3}}^{\frac{2\pi}{3}} i_u d\omega t] \\ = \frac{3}{2\pi}&[I_m (1 + \cos \omega t_1)] \end{aligned} \tag{9}$$

Very interesting, expressions of I_o of RNSIC are same in these three operation modes.

III. PARAMETER DESIGN

A. Operation Mode Selection

The first issue need to be solved in rectifier design is to determine its operation mode, according to the requirement of application field (the input voltage, output voltage and output power).

The input and output power is given as

$$P_{in} = 3\frac{U_m}{\sqrt{2}}\frac{I_m}{\sqrt{2}} = 3\frac{U_m I_m}{2} \tag{10}$$

$$P_o = U_o I_o \tag{11}$$

Where U_o is the output voltage value, neglecting the voltage ripple.

Neglecting the power losses of the converter gives:

$$P_{in} = P_o \tag{12}$$

The relationship between U_o and U_m could be expressed as follow:

$$\frac{U_m}{U_o} = \frac{2I_o}{3I_m} \tag{13}$$

Substituting (7) for I_o/I_m into (13) gives:

$$\frac{U_m}{U_o} = \frac{1+\cos\omega t_1}{\pi} \tag{14}$$

Solving (14) for ωt_1 gives the expression of ωt_1 as a function of U_m and U_o in RNSIC converter.

$$\omega t_1 = \arccos\left(\frac{\pi U_m}{U_o} - 1\right) \tag{15}$$

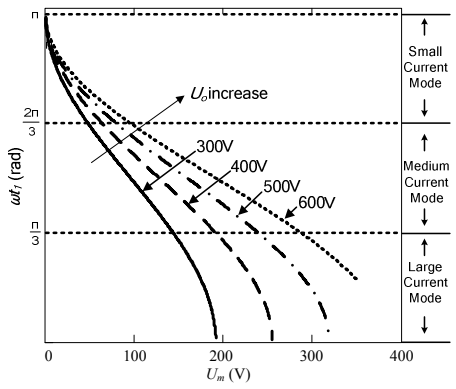

Figure 6. Variations of ωt_1 as a function of U_m and U_o.

Fig. 6 presents the variation of ωt_1 as a function of U_m and U_o in RNSIC converters. For the output voltage U_o, we have adopted the value of 300 V, 400V, 500 V, 600 V. From the analysis given above, which operation mode RNSIC converters work in is determined by t_1. Actually, Fig. 6 gives us the criterion which operation mode RNSIC converters work in.

From this diagram, we could find that RNSIC converters have following characteristic: ① which operation mode RNSIC converters work in is only determined by the input voltage and output voltage, the output power does not affect their operation mode; ② in the application with low input voltage and high output voltage, RNSIC converter should be designed to work in the small current mode, whereas in the application with high input voltage and relatively low output voltage, RNSIC converters suit be designed to work in the large current mode.

B. Time Weighted Averaging Based Parameter Design Method

In this paper, passive components are designed by using time weighted average method. Final optimal parameter value is derived by weighted averaging multiple parameter values which are calculated in different operation stages.

Two distinct operation stages in which different diodes conduct exist in every 1/6 period for RNSIC converter. Moreover, operation stages of RNSIC converter repeat every 1/6 period. So the auxiliary circuit could be designed as follow:

--First, according to the operation mode of RNSIC converter, choose one 1/6 period, calculate the parameter value of auxiliary circuit in two operation stages, respectively.

--Second, obtain the conclusive optimal value by time weighted averaging the two values derived above in 1/6 period.

Take the design of RNSIC working in medium current mode for example.

The relationship between the ac side voltage and current of the rectifiers could be represented by employing KVL law as:

$$e_p + e_u = L\frac{di_u}{dt} + u_M \tag{16}$$

$$e_p + e_v = L\frac{di_v}{dt} + u_N \tag{17}$$

$$e_p + e_w = L\frac{di_w}{dt} + u_F \tag{18}$$

Considering the symmetric of phase voltage, the voltage of neuter point e_p could be expressed as follow:

$$e_p = \frac{u_M + u_N + u_F}{3} \tag{19}$$

1 Operation stage [t_2, t_3]

In the operation stage of [t_2, t_3], diode D_5 keeps conducting, input current i_u keeps charging C_4 and discharging C_1 from zero time point. So the voltage of point

M, *N*, *F* could be expressed as follows:

$$u_M = u_{c4} = \frac{1}{C}\int_0^t \frac{1}{2} I_m \sin \omega t dt = \frac{I_m}{2C\omega}(1-\cos \omega t) \quad (20)$$

$$u_N = 0 \quad (21)$$

$$u_F = U_o \quad (22)$$

Substituting (20) for u_M, (21) for u_N and (22) for u_F into (19) gives:

$$e_p = [\frac{I_m}{2C\omega}(1-\cos \omega t) + 0 + U_o]/3 \quad (23)$$

Subtracting (16) from (17) gives:

$$e_v - e_w = L(\frac{di_v}{dt} - \frac{di_w}{dt}) + (u_N - u_F) \quad (24)$$

Substituting (1) for i_v and i_w, (21) for u_N, and (22) for u_F, into (24) gives:

$$\begin{aligned} e_v - e_w = L[&d(I_M \sin(\omega t - \frac{2\pi}{3}))/dt \\ &- d(I_M \sin(\omega t + \frac{2\pi}{3}))/dt] + (0 - U_o) \end{aligned} \quad (25)$$

Integrating both sides of (25) on the angel interval [ωt_2, ωt_3] and simplifying gives the value of optimal inductance as follow:

$$L_1 = \frac{\int_{\omega t_1 - \frac{\pi}{3}}^{\frac{\pi}{3}} (e_w - e_v - U_o) d\omega t}{I_m \omega[-\sin(\omega t_1 + \frac{\pi}{3}) - \sin \omega t_1 + \frac{\sqrt{3}}{2}]} \quad (26)$$

Here, ωt_2 corresponds to ωt_1-π/3, ωt_3 corresponds to π/3.

Substituting (21) for u_N, and (23) for e_p into (17) gives:

$$[\frac{I_m}{6C\omega}(1-\cos \omega t) + \frac{U_o}{3}] + e_v = L_1 \frac{di_v}{dt} + 0 \quad (27)$$

Integrating both sides of (27) on the angle internal [ωt_2, ωt_3] and simplifying gives the expression of C_1:

$$\begin{aligned} C_1 = &\int_{\omega t_1 - \frac{\pi}{3}}^{\frac{\pi}{3}} I_m (1-\cos \omega t) d\omega t / 6\omega[L_1 \omega I_m (\sin \omega t_1 \\ &- \frac{\sqrt{3}}{2}) - \frac{U_o}{3}(-\omega t_1 + \frac{2\pi}{3}) - \int_{\omega t_1 - \frac{\pi}{3}}^{\frac{\pi}{3}} e_v d\omega t] \end{aligned} \quad (28)$$

2 Operation stage [t_3, t_1]

In the operation stage of [t_3, t_1], input current i_u keeps charging C_4 and discharging C_1, diode D_6 keeps conducting So the voltage of point *M* and *N* have the same expression with the one in the last stage and the voltage of point *F* could be expressed as follows:

$$\begin{aligned} u_F = u_{c2} &= u_{c2}\big|_{t=t_3} + \frac{1}{C}\int_{t_3}^t \frac{1}{2} I_m (\sin \omega t + \frac{2}{3}\pi) dt \\ &= U_o - \frac{I_m}{2C\omega}(1 + \cos(\omega t + \frac{2\pi}{3})) \end{aligned} \quad (29)$$

Equ. (23) should be modified as follow:

$$e_p = \frac{1}{3}[\frac{-I_m}{2C\omega}(\cos(\omega t + \frac{2\pi}{3}) + \cos \omega t) + U_o] \quad (30)$$

After obtaining the voltage of point e_p and u_F, optimal inductance and capacitance in the stage of [t_3, t_1] could be derived by using the above similar method. Expression C_2 of and L_2 are derived as follow:

$$C_2 = \frac{\int_{\frac{\pi}{3}}^{\omega t_1} I_m [1 + \cos(\omega t + \frac{2\pi}{3})] d\omega t}{3\omega[\int_{\frac{\pi}{3}}^{\omega t_1} (\frac{2U_o}{3} + e_v) d\omega t + I_m L_1 \omega \sin(\omega t_1 - \frac{2\pi}{3})]} \quad (31)$$

$$\begin{aligned} L_2 = &\{\int_{\frac{\pi}{3}}^{\omega t_1} (e_v - e_w + U_o) d\omega t - \int_{\frac{\pi}{3}}^{\omega t_1} \frac{3[1 + \cos(\omega t + \frac{2\pi}{3})]}{\sin \omega t_1 + \sin(\omega t + \frac{2\pi}{3}) - \frac{\sqrt{3}}{2}} \cdot \\ &[U_m(\frac{1}{2} - \cos(\omega t_1 - \frac{2\pi}{3})) + \frac{U_o}{3}(\omega t_1 - \frac{\pi}{3})] d\omega t)\} / \{I_m \omega[\sin(\omega t_1 - \\ &\frac{2\pi}{3}) - \sin(\omega t_1 + \frac{2\pi}{3}) + \frac{\sqrt{3}}{2}] - \int_{\frac{\pi}{3}}^{\omega t_1} \frac{3 I_m \omega [1 + \cos(\omega t + \frac{2\pi}{3})]}{\sin \omega t_1 + \sin(\omega t + \frac{2\pi}{3}) - \frac{\sqrt{3}}{2}} \cdot \\ &[\sin(\omega t_1 - \frac{2\pi}{3}) + \frac{\sqrt{3}}{2}] d\omega t\} \end{aligned} \quad (32)$$

Optimal inductance and capacitance are derived as follows:

$$L = \frac{L_1(\frac{2\pi}{3} - \omega t_1) + L_2(\omega t_1 - \frac{\pi}{3})}{\frac{\pi}{3}} \quad (33)$$

$$C = \frac{C_1(\frac{2\pi}{3} - \omega t_1) + C_2(\omega t_1 - \frac{\pi}{3})}{\frac{\pi}{3}} \quad (34)$$

IV. EXPERIMENTAL VERIFICATION

In order to verify the feasibility of the analysis and the proposed design method, three prototype systems working in different modes were built with the following specification (as Tab.1 shown).

Fig. 7 shows the experimental waveforms of the phase voltage and input current of the prototypes working in the large current mode, medium current mode and small current mode, respectively. It can be seen that the input currents are practically sinusoidal and the displacement factor is near unity.

TABLE I. SPECIFICATION OF THREE RNSIC PROTOTYPES

Prototype	U_m / V	U_o / V	P_o / kW	L / mH	C / μF	Operation Mode
1	250	500	7.18	27.7	22.46	large current mode
2	150	500	6.55	27.7	98.7	Medium current mode
3	55	500	2.52	27.7	159.2	small current mode

Fig. 8 shows the spectrum of the input current of the three prototypes, where the THDs are 4.916%, 5.042%, 5.643%, respectively.

CONCLUSION

The RNSIC converter catches increasing attention for its simple configuration, high reliability as well as the reduced cost. This paper has proposed a practical design method of the RNSIC on the basis of operation principle analysis. Experimental results that the THD lower than 10% and power factor higher than 0.99, which are obtained from three prototypes work with different modes have verified both the validity of theoretical analysis and the feasibility of the design method.

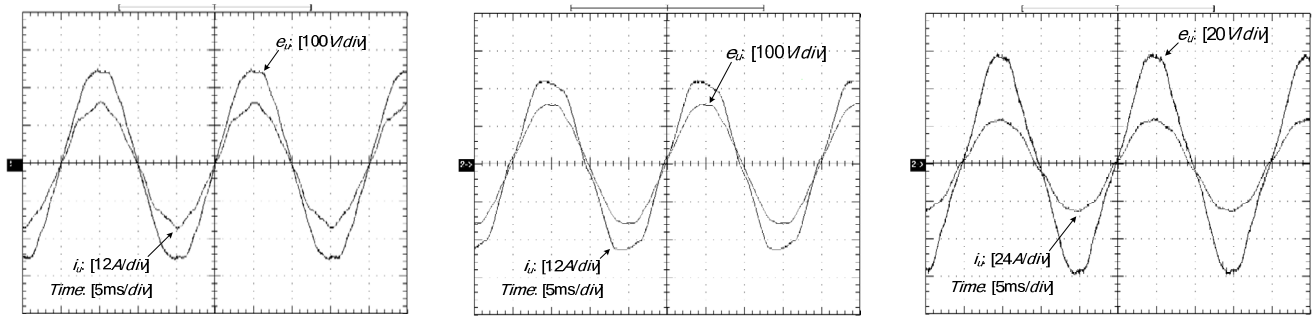

(a) Prototype 1 (b) Prototype 2 (c) Prototype 3

Figure 7. Experimental waveforms of phase voltage $e_u(t)$ and current $i_u(t)$.

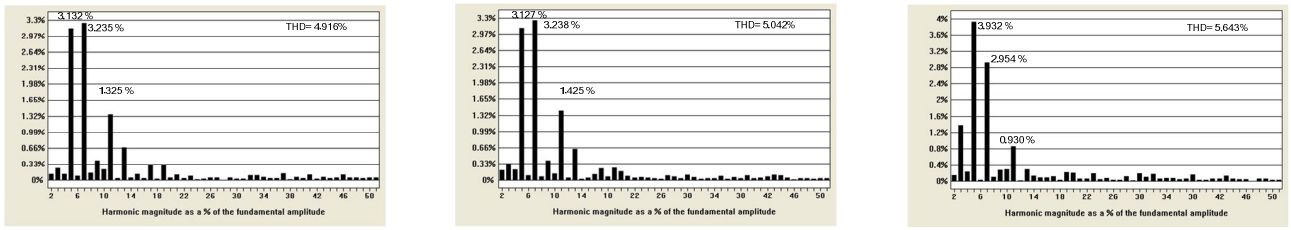

(a) Prototype 1 (b) Prototype 2 (c) Prototype 3

Figure 8. Nomilized line current harmonics of experimental prototypes.

REFERENCES

[1] H. Akagi, E. H. Watanabe, and M. Aredes, Instantaneous Power Theory and Applications to Power Conditioning, New Jersey: John Willey & Sons, 2007, pp. 4-5.

[2] H. Akagi, "The state-of-the-art of active filters for power conditioning," EPE 2005-11th European Conference on Power Electronics and Applications, 2005, pp. 1-15.

[3] A. W. Kelley and W. F. Yadusky, "Rectifier Design for Minimum Line-Current Harmonics and Maximum Power Factor," IEEE Trans. Power Electronics, Vol. 7, No. 2, pp. 663-672, Apr. 1992.

[4] M. Sakui and H. Fujita, "An Analytical Method for Calculating Harmonic Current of a Three-phase Diode bridge Rectifier with dc Filter," IEEE Trans. Power Electronics, Vol. 9, No. 6, pp. 631-637, Nov. 1994.

[5] B. Singh, G. Bhuvaneswari, and V. Garg, "T-Connected Autotransformer - Based 24-Pulse AC-DC Converter for Variable Frequency Induction Motor Drives," IEEE Trans. Energy Conversion, Vol. 21, No. 3, pp. 663-672, Sep. 2006.

[6] R. P. Burgos, A. Uan-Zo-li, F. Lacaux, A. Roshan, F. Wang, and D. Boroyevich, "Analysis of New Step-Up and Step-Down 18 Pulse Direct Asymmetric Autotransformer Rectifiers," in Proc. IEEE Conf. IAS, 2005, Vol. 1, pp. 145–152.

[7] F.J.M. de Seixas and I. Barbi, "A 12kW three-phase low THD rectifier with high frequency isolation and regulated dc output," IEEE Trans. Power Electronics, Vol. 19, No. 2, pp. 371-377, Mar. 2004.

[8] P. Pejović, P. Božović, and D. Shmilovitz, "Low-Harmonic, Three-Phase Rectifier That Applies Current Injection and a Passive Resistance Emulator," IEEE Power Electronics Letters, Vol. 3, No. 3, pp. 96-100, Sep. 2005.

[9] P. Pejović and Z. Janda, "An Analysis of Three-Phase Low Harmonic Rectifiers Applying the Third-Harmonic Current Injection," IEEE Trans. Power Electronics , Vol. 14, No. 3, pp. 397-407, May 1999.

[10] I. Yamamoto, K. Ohtsuka, K. Matsui, and Y. Yao, "A Novel Three-Phase Diode Rectifier with LC Resonance in Commercial Frequency," in Proc. IEEE IECON'01 Conf., 2001, pp. 1350-1356.

[11] D. Alexa and A. Sîrbu, "Optimized Combined Harmonic Filtering System," IEEE Trans. Industrial Electronics, Vol. 48, No. 6, pp. 1210-1218, Dec. 2001.

[12] D. Alexa, A. Sîrbu, and D. Dobrea, "Topologies of Three-Phase Rectifiers with Near Sinusoidal Input Currents," in Proc. IEE Electr. Power Appl., Vol. 151, No. 6, pp. 673-678, Nov. 2004.

[13] D. Alexa, A. Sîrbu, and D. Dobrea, "An Analysis of Three-Phase Rectifiers with Near-Sinusoidal Input Current," IEEE Trans. Industrial Electronics, Vol. 51, No. 4, pp. 884-891, Aug. 2004.

[14] D. Alexa, A. Sîrbu, and A. Lazăr, "Three-Phase Rectifiers with Near Sinusoidal Input Current and Capacitors Connected on the AC side," IEEE Trans. Industrial Electronics, Vol. 53, No. 5, pp. 1612-1620, Oct. 2006